ALTERNATIVE PROCEDURES FOR THE INCORPORATION OF LIDAR-DERIVED LINEAR AND AREAL FEATURES FOR PHOTOGRAMMETRIC GEO-REFERENCING

A.F. Habib, M. Aldelgawy[a]

[a] Department of Geomatics Engineering, University of Calgary, Canada
habib@geomatics.ucalgary.ca, mmaldelg@ucalgary.ca

WG I/2 WG I/2 - SAR and LiDAR Systems

KEY WORDS: Digital Photogrammetry, Digital Orthophoto, Aerial Photogrammetry, Adjustment, Land Use Mapping, LiDAR, Linear Features, Areal Features

ABSTRACT:

The positional and spectral information in LiDAR and photogrammetric data are optimal for providing a complete description of 3D environments. However, the synergistic attributes of the LiDAR and photogrammetric data can be only achieved after their proper registration to a common reference frame. This paper presents alternative methodologies for utilizing LiDAR-derived features for geo-referencing the photogrammetric data relative to the LiDAR reference frame. Since the LiDAR footprints are irregularly distributed, no point-to-point correspondence can be assumed between the photogrammetric and LiDAR data. In other words, it is almost impossible to identify distinct conjugate points in overlapping photogrammetric and LiDAR data. Consequently, LiDAR linear and areal features will be used as control information for the geo-referencing of the photogrammetric data. The paper will present three alternative methodologies to solve this task. The first approach outlines constraints that can be added to current bundle adjustment procedures to incorporate LiDAR linear and areal features. The second approach utilizes existing point-based bundle adjustment procedures for the incorporation of linear and areal features after manipulating the variance-covariance matrices associated with the points representing these features. Finally, the third approach will be based on weight restrictions imposed on the points representing the linear and areal features. After the introduction of the proposed methodologies, the paper will proceed by discussing experimental results using simulated datasets through a root mean square error analysis of a number of check points.

1. INTRODUCTION

Considering the characteristics of acquired spectral and spatial data from imaging and LiDAR systems, one can argue that their integration will be beneficial for accurate and complete description of the object space. It is evident that the disadvantages of one system can be compensated for by the advantages of the other system (Baltsavias, 1999; Satale and Kulkarni, 2003). However, the synergic characteristics of both systems can be fully utilized only after ensuring that both datasets are geo-referenced relative to the same reference frame (Habib and Schenk, 1999). Traditionally, photogrammetric geo-referencing is either indirectly established with the help of ground control points (GCP) or directly defined using GPS/INS units on board the imaging platform (Cramer et al, 2000). On the other hand, LiDAR geo-referencing is directly established through the GPS/INS components of a LiDAR system. In this regard, this paper presents alternative methodologies for utilizing LiDAR features as a source of control for photogrammetric geo-referencing. There are various techniques dealing with linear and areal features in photogrammetry (Habib et al, 2007). Three approaches are presented in this research. The first one outlines a constraint that should be added to the current bundle adjustment procedures, while the second and third ones utilize the existing point-based bundle adjustment procedures for the incorporation of linear and areal features. The second approach manipulates the variance-covariance matrices associated with the points representing image and/or object space linear features, and the third one manipulates the weight matrices.

The paper introduces the different approaches for incorporation of both linear and areal features for image geo-referencing as well as experimental results and analysis in the following sections. Section 2 discusses the incorporation of linear features. The coplanarity-based incorporation of linear features is discussed in sub-section 2.1. Sub-section 2.2 explains the point-based incorporation of linear features. The error ellipse expansion and the weight restriction methodologies are discussed in sub-sections 2.2.1 and 2.2.2 respectively. An illustration of the applications of the point-based approaches for linear features is shown in sub-section 2.2.3. Afterwards, the incorporation of areal features is illustrated in section 3. The coplanarity-based incorporation of planar patches is shown in sub-section 3.1. Sub-section 3.2 outlines the point-based approaches for incorporation of planar patches. The error ellipse expansion and the weight restriction approaches for planar patches are illustrated in sub-sections 3.2.1 and 3.2.2, respectively. In addition, experimental results and analysis for simulated dataset are discussed in section 4. Experiments for both single photo resection and bundle adjustment are shown in sub-sections 4.1 and 4.2, respectively. Finally, the conclusions and recommendations for future work are summarized in section 5.

2. INCORPORATION OF LINEAR FEATURES FOR IMAGE GEO-REFERENCING

This section presents the approaches used for incorporating linear features extracted from LiDAR data for the geo-referencing of photogrammetric data. The first approach is the coplanarity-based incorporation of linear features, while the second one is the point-based incorporation of linear features, where we can either expand the error ellipse or restrict the weight matrix. These approaches are provided in details in the

following sub-sections.

2.1. Coplanarity-Based Incorporation of Linear Features

The coplanarity-based incorporation of linear features was presented by Habib et al, 2004. This technique defines a line in object space by two end points. These two points are extracted from the LiDAR data. On the other hand, the line is defined in image space by a group of intermediate points. Each of the intermediate points satisfies the coplanarity constraint equation in the following form:

$$\left(\vec{V}_1 \times \vec{V}_2\right) \bullet \vec{V}_3 = 0 \qquad (1)$$
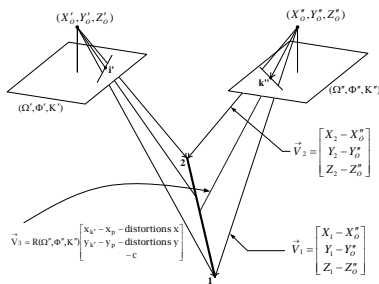

Figure 1: Coplanarity constraint for lines

The constraint in equation 1 indicates that the vector $\vec{V}_1$ from the perspective center *(X_o, Y_o, Z_o)* to the first LiDAR end point of the line *(X_1, Y_1, Z_1)*, the vector $\vec{V}_2$ from the perspective center to the second LiDAR end point of the line *(X_2, Y_2, Z_2)*, and vector $\vec{V}_3$ from the perspective center to any intermediate image point are coplanar. In other words, for a given intermediate point, k″, the points {*(X_1, Y_1, Z_1)*, *(X_2, Y_2, Z_2)*, *(X″_0, Y″_0, Z″_0)*, and *(x_{k″}, y_{k″}, 0)*} lie on the same plane (Figure 1).

It should be noted that the above constraint can be introduced for all the intermediate points along image space linear features. Moreover, the coplanarity constraint is valid for both frame and line cameras. For frame cameras with known interior orientation parameters (IOP), a maximum of two independent constraints can be defined for a given image. However, for self-calibration procedures, additional constraints will help in the recovery of the IOP since the distortion pattern will change from one intermediate point to the next along image space linear features. On the other hand, the coplanarity constraint would help in better recovery of the exterior orientation parameters (EOP) associated with line cameras. Such a contribution is attributed to the fact that the system's trajectory will affect the shape of linear features in image space. For scenes captured by line cameras, the involved EOP should correspond to the image associated with the intermediate point under consideration.

2.2. Point-Based Incorporation of Linear Features

A new technique is presented here for the incorporation of linear features in photogrammetric triangulation. This technique uses a point-based approach in which a line is defined by two points in image space and two LiDAR points in object space. Correspondence between image and object space points along the linear features is not necessary (Figure 2). The approach is based on expanding the error ellipse or restricting the weight matrix in the line direction for the (two) points lying on this line. Consequently, the behavior of these points will be fixed in all

directions except for the line direction. This means that the point is free to move only along the line, which is considered as a constraint. The following collinearity equations are the used mathematical model:

$$x = -c\left(\frac{m_{11}(X - X_o) + m_{12}(Y - Y_o) + m_{13}(Z - Z_o)}{m_{31}(X - X_o) + m_{32}(Y - Y_o) + m_{33}(Z - Z_o)}\right) + x_p + \Delta x \qquad (2)$$

$$y = -c\left(\frac{m_{21}(X - X_o) + m_{22}(Y - Y_o) + m_{23}(Z - Z_o)}{m_{31}(X - X_o) + m_{32}(Y - Y_o) + m_{33}(Z - Z_o)}\right) + y_p + \Delta y \qquad (3)$$

Where,

(x, y) are the point coordinates in image space,

(X, Y, Z) are the point coordinates in object space,

(x_p, y_p, c) are the principal point coordinates and principal distance,

$(\Delta x, \Delta y)$ are the distortion parameter effects in the (x, y) image coordinates,

(X_O, Y_O, Z_O) are the coordinates of the camera perspective center with respect to the object coordinate system,

$$M(\omega, \phi, \kappa) = \begin{bmatrix} m_{11} & m_{12} & m_{13} \\ m_{21} & m_{22} & m_{23} \\ m_{31} & m_{32} & m_{33} \end{bmatrix}$$

is the rotation matrix from the object coordinate system to the image coordinate system.

Two alternatives can be used for the point-based technique. The first one is expanding the error ellipse, variance-covariance matrix, in the line direction, and the second one is restricting the weight matrix in the line direction. These two alternatives are discussed in the following sub-sections.
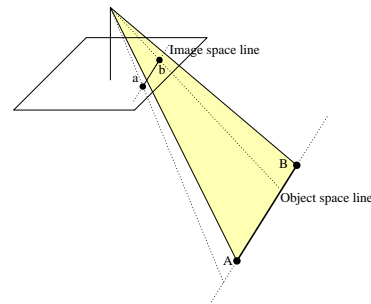

Figure 2: Representation of image and object lines for the point-based incorporation of linear features

2.2.1. Variance-covariance matrix expansion in the line direction

Variance-covariance matrix expansion can be accomplished in image space or in object space. One should note that the only difference between the two is the matrix size — 2x2 in image space and 3x3 in object space. The approach of error ellipse expansion in object space proceeds as follows:

(1) Define a line by any two points *A* and *B* lying on it.

(2) Define the rotation matrix, R, to transform the points'

coordinates from the original coordinate system (X, Y, Z) to the line coordinate system (U, V, W), where the U axis is in the line direction (Figure 3.a).

(3) Compute the variance-covariance matrix in the line coordinate system, Σ_{UVW}, for each of the two points A and B using the law of error propagation:

$$\sum\nolimits_{UVW} = R \sum\nolimits_{XYZ} R^T \qquad (4)$$

where Σ_{XYZ} is the variance-covariance matrix in the (X, Y, Z) coordinate system (Figure 3.b,c),

(4) Assign a large value for the variance in the line direction by applying a large scaling factor, m, (Figure 3.d):

$$\sigma'_U = m\,\sigma_U$$

Then, the new variance-covariance in the (U, V, W) coordinate system, $\sum\nolimits'_{UVW}$ will be as follows:

$$\sum\nolimits'_{UVW} = \begin{bmatrix} \sigma'^2_U & \sigma_{UV} & \sigma_{UW} \\ \sigma_{VU} & \sigma^2_V & \sigma_{VW} \\ \sigma_{WU} & \sigma_{WV} & \sigma^2_W \end{bmatrix} \qquad (5)$$

(5) Again, rotate the variance-covariance matrix to the original system (X, Y, Z) and compute the new $\sum\nolimits'_{XYZ}$ as follows:

$$\sum\nolimits'_{XYZ} = R^T \sum\nolimits'_{UVW} R \qquad (6)$$

(6) Apply a point-based solution using the two collinearity equations 2 and 3 with the new $\sum\nolimits'_{XYZ}$

a) Line coordinate system (U, V, W)

b) Original error ellipse in (X, Y, Z) coordinate system

c) Error ellipse in (U, V, W) coordinate system

d) Error ellipse in (U, V, W) coordinate system after expanding the variance-covariance matrix in the line direction
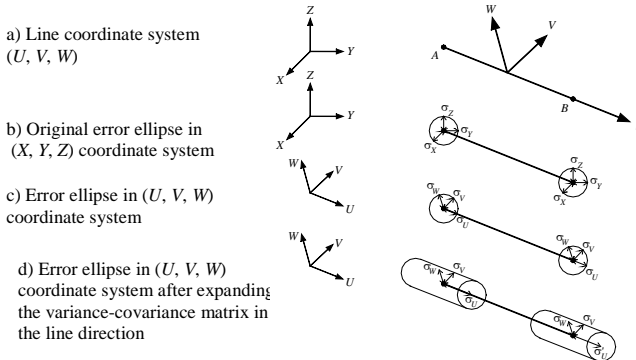
Figure 3: Expanding the error ellipse in the line direction

2.2.2. Weight matrix restriction in the line direction

This approach is similar to the previous one except that instead of a variance expansion a weight restriction is applied, i.e. the weights of points along the linear features are set to zero. The weight matrix restriction can be done in either image or object spaces. In image space, we use a 2x2 weight matrix, while in object space, weight matrix is 3x3. An explanation of the 3x3 weight matrix restriction in object space is introduced as

follows:

(1) Compute the weight matrix in the line coordinate system as follows:

$$P_{UVW} = R\,P_{XYZ}\,R^T \qquad (7)$$

Where:
P_{XYZ} is the weight matrix in the object coordinate system
P_{UVW} is the weight matrix in the line coordinate system

(2) Assign a zero value for the weights in the line direction; i.e.:

$$P'_{UVW} = \begin{bmatrix} 0 & 0 & 0 \\ 0 & p_v & p_{vw} \\ 0 & p_{wv} & p_w \end{bmatrix} \qquad (8)$$

(3) Rotate the weight matrix to the original (X, Y, Z) system computing the new P'_{XYZ} as follows,

$$P'_{XYZ} = R^T\,P'_{UVW}\,R \qquad (9)$$

(4) Apply a point-based solution using a least squares adjustment with the new P'_{XYZ}.

2.2.3. Applications of point-based approaches for linear features

In the this sub-section, the focus will be on the photogrammetric applications of the point-based approach for lines using both frame and line cameras by expanding the error ellipse, or restricting the weight matrix, in the image or object space. The incorporation of linear features in photogrammetric triangulation will proceed as follows:

(1) Single Photo Resection Using Control Lines:
In the case of single photo resection, the error ellipse expansion, or weight restriction, can be applied in object space or in image space. When expanding the error ellipse, or restricting the weight matrix, in object space (Figure 4.a), the image line will be represented by two end points with their variance-covariance matrices defined by the expected image coordinate measurement accuracy. On the other hand, the variance-covariance matrices of the end points of the object line are expanded to compensate for the fact that the image and object points are not conjugate. It should be noted that it does not matter if we use frame or line cameras.

When expanding the error ellipse, or restricting the weight matrix, in image space (Figure 4.b), the object line will be represented by its end points, whose variance-covariance matrices are defined by the expected accuracy of the utilized procedure for defining these points. On the other hand, the variance-covariance matrices of the points along the image line are expanded along its direction. It should be noted that we can expand the error ellipse, or restrict the weight matrix, only in case of using calibrated frame cameras. For scenes captured by line camera, this approach is not appropriate since the image-line orientation cannot be rigorously defined at a given point

due to perturbations in the flight trajectory. However, the line orientation along the scene can be used as an approximation.

(2) Bundle Adjustment Using Control Lines:
In this case, the error ellipse expansion, or weight restriction, can be applied in either image or object space. When expanding the error ellipse, or restricting the weight matrix, in image space (Figure 4.c), the object line will be represented by its end points with their variance-covariance matrices defined by the utilized procedure for providing the control lines. On the other hand, the variance-covariance matrices of the image lines are expanded, the weight matrices are restricted, to compensate for the fact that the end points of the image lines are not conjugate to those defining the object line. It should be noted that this approach is not appropriate for scenes captured by line cameras since the image line orientation cannot be rigorously defined.

When expanding the error ellipse, or restricting the weight matrix, in object space (Figure 4.d), the image lines will be represented by non-conjugate end points whose variance-covariance matrices are defined by the expected accuracy of the image coordinate measurements. To compensate for the fact that these points are not conjugate to each other, the selected end points will be assigned different identification codes. On the other hand, the object line will be defined by a number of points whose variance-covariance matrices are expanded, or weight matrices are restricted. If we have m images, the number of these points will be $2m$ since every line is defined by two points. It should be noted that this approach can be used for scenes captured by frame or line cameras since it does not require the expansion of the variance-covariance matrix, or the restriction of the weight matrix, in image space.
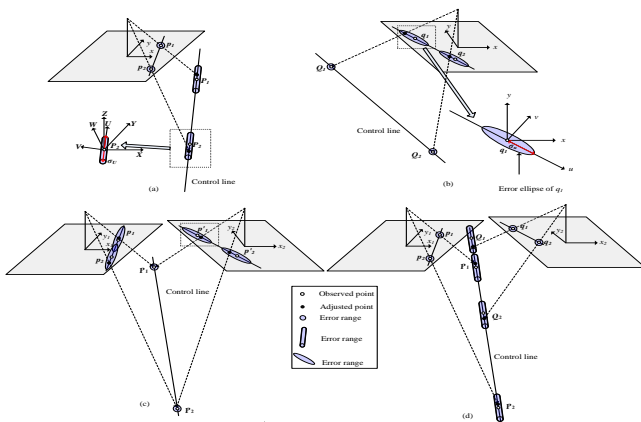

Figure 4: Variance expansion and weight restriction options of line end points for their incorporation in point-based bundle adjustment procedures

3. INCORPORATION OF AREAL FEATURES IN PHOTOGRAMMETRY

The approaches used to incorporate areal features extracted from LiDAR data in photogrammetric triangulation are presented in this section. The first approach is the coplanarity-based incorporation of areal features, while the second one is the point-based incorporation of areal features, where we can either expand the error ellipse or restrict the weight matrix. The following sub-sections explain these approaches in details.

3.1. Coplanarity-Based Incorporation of Planar Patches

In this approach, the planar patch is defined by three points, a, b, and c in image space and a set of LiDAR points in object space (Habib, A. et al, 2007). The points, a, b, and c should be observed in at least two overlapping images (Figure 5). The collinearity equations 2 and 3 are used to relate the image space coordinates (x, y) to the object space coordinates (X, Y, Z) for the image points a, b, c. For any LiDAR point P in object space, the following constraint should be satisfied:

$$V = \begin{vmatrix} X_P & Y_P & Z_P & 1 \\ X_A & X_A & X_A & 1 \\ X_B & X_B & X_B & 1 \\ X_C & X_C & X_C & 1 \end{vmatrix} = \begin{vmatrix} (X_P - X_A) & (Y_P - Y_A) & (Z_P - Z_A) \\ (X_B - X_A) & (Y_B - Y_A) & (Z_B - Z_A) \\ (X_C - X_A) & (Y_C - Y_A) & (Z_C - Z_A) \end{vmatrix} = 0 \quad (10)$$

where, $(X, Y, Z)_{A,B,C}$ are the object space coordinates of image points a, b, c and (X_P, Y_P, Z_P) are the object space coordinates of any ground point, $P = 1$ to n, where n is the number of extracted LiDAR points in the areal feature.

The above constraint in equation 10 is used as the mathematical model for incorporating LiDAR points into the photogrammetric triangulation. In physical terms, this constraint means that the normal distance between any LiDAR point P and the corresponding photogrammetric surface consisting of the three points A, B, C should be zero. In other words, the volume of the tetrahedron comprised of the four points is equal to zero as these four points belong to the same plane. This constraint is applied for all LiDAR points comprising this surface patch.
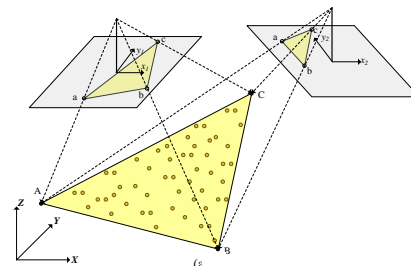

Figure 5: Coplanarity-based incorporation of planar patches

3.2. Point-Based Incorporation of Planar Patches

A new approach to incorporate the planar patches using a point-based technique is presented here. In this case, conjugate patch vertices are defined in at least two overlapping images. Then, an equal number of patch vertices is defined in object space. Correspondence between points in image space and object space is not necessary (Figure 6). The used mathematical model is the regular collinearity equations 2 and 3. To compensate for the fact that there is no correspondence of points between image and object spaces, we expand the error ellipse, or restrict the weight matrix, in object space. Variance expansion, or weight restriction, in image space is not applicable since all patches in image space belong to the same 2-D plane (i.e. the image itself). Two alternatives of the point-based techniques are used. The first one relies on expanding the error ellipse, variance-covariance matrix, along the areal feature, while the second one relies on restricting the weight matrix along the areal feature. Since the error expansion, or weight restriction, is done only in object space, this approach is valid for both frame and line cameras.
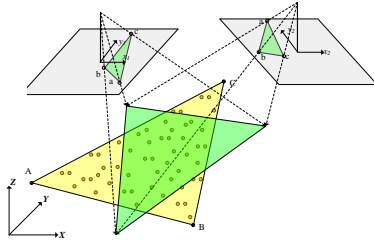
Figure 6: Point-based incorporation of planar patches

3.2.1. Variance-covariance expansion for planar patches

Variance expansion in object space is done as follows:
(1) Define the patch by three points, *A*, *B*, and *C* belonging to it in object space.
(2) Compute the rotation matrix, *R*, to relate the variance co-variance matrix in the original coordinate system (*X*, *Y*, *Z*) to the variance co-variance matrix in the patch coordinate system (*U*, *V*, *W*), where the *U* and *V* axes are within the patch plane and the *W* axis is normal to it (Figure 7.a).
(3) Compute the variance-covariance matrix in the patch coordinate system, Σ_{UVW}, for the three points *A*, *B*, and *C* using the law of error propagation:

$$\sum_{UVW} = R \sum_{XYZ} R^{T} \tag{11}$$

where Σ_{XYZ} is the variance-covariance matrix in the *(X, Y, Z)* coordinate system (Figure 7.b).

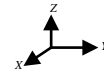(4) Assign a large value for the variance in the plane direction by applying a large scaling factor, *m* (Figure 7.c):

$$\sigma'_{U} = {}^{m}\sigma_{U} , \ \sigma'_{V} = {}^{m}\sigma_{V}.$$

Then, the new variance-covariance matrix in the (*U*, *V*, *W*) coordinate system, $\sum'_{UVW}$, will be as follows:
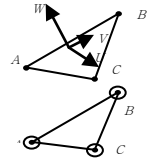
$$\sum{}'_{UVW} = \begin{bmatrix} \sigma'^{2}_{U} & \sigma_{UV} & \sigma_{UW} \\ \sigma_{VU} & \sigma'^{2}_{V} & \sigma_{VW} \\ \sigma_{WU} & \sigma_{WV} & \sigma^{2}_{W} \end{bmatrix} \tag{12}$$

(5) Rotate the variance-covariance matrix to the original (*X, Y, Z*) system computing the new $\sum'_{XYZ} = R^{T} \sum'_{UVW} R$.

(6) Apply a point-based solution using the two collinearity equations 2 and 3 while considering the modified variance-covariance matrix, $\sum'_{XYZ}$, for the points.

a) Patch coordinate

b) Original error ellipse in (*X*, *Y*, *Z*) coordinate system

c) Error ellipse in (*U*, *V*, *W*) coordinate system after expanding the variance in the patch direction
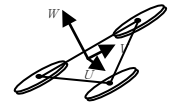

Figure 7: Expanding the error ellipse in the patch plane

3.2.2. Weight restriction for planar patches

This approach is similar to the one in sub-section 3.2.1 except that instead of a variance expansion a weight restriction is applied, i.e. the weights for points along areal features are set to zero. The procedure is as follows:
(1) Define an areal feature by any three points *A*, *B*, *C* lying on it.
(2) Compute the weight matrix along the planar patch as follows:

$$P_{UVW} = R \ P_{XYZ} R^{T} \tag{13}$$

Where P_{XYZ}, P_{UVW} are the weight matrices in the object and patch coordinate systems, respectively.
(3) Assign a zero value for the weights along the patch plane:

$$P'_{UVW} = \begin{bmatrix} 0 & 0 & 0 \\ 0 & 0 & 0 \\ 0 & 0 & p_{W} \end{bmatrix} \tag{14}$$

Therefore,
$$P'_{XYZ} = R^{T} P'_{UVW} R \tag{15}$$

(4) Apply a point-based solution using a least squares solution with the modified weight matrix, P'_{XYZ} .

4. EXPERIMENTAL RESULTS

Experimental work was conducted to validate the feasibility and applicability of the above approaches using simulated data. The simulation model consists of a group of buildings covering an area of 7000 x 7700 square meters. All buildings have planimetric dimensions of 10 x 10 meters with different heights and roof angle of 20 degrees (Figure 8). The spacing between LiDAR footprints was chosen as 0.500 meters in the planimetric direction (*X*, *Y* directions).
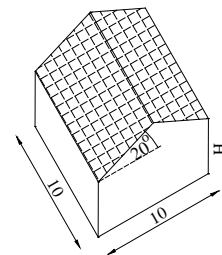

Figure 8: Isometric view of a sample building

A simulated camera was assumed to capture all the photographs (Table 1). Six synthetic photographs with normal geometric con

figuration, which represents the case of aerial photography, wer e generated for the experimentation. The six photos are captured in two strip lines (each strip consists of three photos). The exter ior orientation parameters of the six camera stations are listed in Table 2. The base distance to flying height ratio was 0.8. The i mage coordinates (x, y) for each object point were computed fro m the camera parameters and the ground coordinates of this poi nt using the collinearity condition equations (Equations 2, 3). T hen, the perturbed data set was generated with LiDAR planimetr ic standard deviation (in the X, Y directions) of 0.300 meters an d the vertical (in Z direction) standard deviation of 0.100 meters . On the other hand, the image standard deviation was chosen as 6 microns, which resulted in expected accuracy in the object co ordinate system of 0.300 meters in the *X, Y* directions and 0.530 meters in the *Z* direction.

Format Size *(mm)*	100 x 100	x_o *(mm)*	0.018
f (mm)	50	y_o *(mm)*	-0.015

Table 1: Specifications of the simulated camera

Parameter	Nor1	Nor2	Nor3	Nor4	Nor5	Nor6
ω (deg)	0.5	-0.5	1.5	2.0	-1.0	0.5
ϕ (deg)	0.5	0.5	-0.5	1.0	0.5	0.5
κ (deg)	1.5	1.0	-1.0	1.0	1.5	1.5
X_C (m)	1500	3500	5500	1500	3500	5500
Y_C (m)	1850	1850	1850	5600	5600	5600
Z_C (m)	2600	2600	2600	2600	2600	2600

Table 2: Exterior orientation parameters of simulated photos

In all experiments, the used approaches were as follows:
- Control Lines:
  (1) *Model 1*: Coplanarity Constraint for Lines.
  (2) *Model 2*: Variance-Covariance Expansion in Image Space.
  (3) *Model 3*: Variance-Covariance Expansion in Object Space.
  (4) *Model 4*: Weight Restriction in Image Space.
  (5) *Model 5*: Weight Restriction in Object Space.
- Control Patches:
  (6) *Model 6*: Coplanarity Constraint for Planar Patches.
  (7) *Model 7*: Variance-Covariance Expansion in Object Space.
  (8) *Model 8*: Weight Restriction in Object Space.

Experiments were conducted to simulate the case of single photo resection using linear features as well as bundle adjustment using both linear and areal features extracted from LiDAR data applying these eight models as illustrated in the following sub-sections.

4.1 Experiments for Single Photo Resection

In this sub-section, experiments were conducted to simulate the case of single photo resection using control lines applying the models for linear features (*Model 1* to *Model 5*). The single photo resection process was performed to solve for the *EOP* of the photo. The *IOP* of the photo were considered as known parameters, which simulates the case of calibrated frame camera. Single photo resection was conducted twice on two photos to evaluate the solution by performing an intersection process for a set of check points lying on the overlapping area between these two photos. In other words, the single photo resection experiments were conducted on photo Nor1 using 11 control

lines. Then, the experiments were conducted on photo Nor2 using 11 control lines. After solving for the *EOP* for each of the two used photos separately, the ground coordinates of a set of 15 check points were computed. Then, the solution was evaluated through root mean square error (*RMSE*) analysis of these15 check points. Results are summarized in Table 3 where we can find all used five models resulted in reliable and comparable results.

Model No.	Model1	Model2	Model3	Model4	Model5
$RMSE_X$ *(m)*	0.276	0.292	0.358	0.305	0.358
$RMSE_Y$ *(m)*	0.344	0.312	0.346	0.322	0.346
$RMSE_Z$ *(m)*	0.408	0.372	0.456	0.404	0.456
$RMSE_{Total}$ *(m)*	0.600	0.566	0.675	0.600	0.675

Table 3: *RMSE* analysis for single photo resection using linear features for the 15 check points

4.2 Experiments for Bundle Adjustment

Experiments here were conducted to simulate the case of bundle adjustment using both linear and areal features extracted from LiDAR data. The number of control lines was 16 lines. The number of control patches was 32 patches. In all experiments using both linear and areal features, the number of tie points was 35 points. To evaluate the solution, a root mean square error analysis was performed considering the 35 tie points as check points. Results are illustrated in Table 4.

Model No.	Model1	Model2	Model3	Model4	Model5	Model6	Model7	Model8
$RMSE_X$ *(m)*	0.350	0.350	0.383	0.350	0.388	0.349	0.365	0.365
$RMSE_Y$ *(m)*	0.440	0.440	0.514	0.440	0.517	0.416	0.414	0.417
$RMSE_Z$ *(m)*	0.529	0.522	0.628	0.522	0.637	0.487	0.494	0.486
$RMSE_{Total}$ *(m)*	0.772	0.767	0.897	0.767	0.908	0.729	0.740	0.737

Table 4: *RMSE* analysis for bundle adjustment using both linear and areal features for the 35 check points

Table 4 shows a comparison between the values of $RMSE_X$, $RMSE_Y$, $RMSE_Z$ and $RMSE_{Total}$ for the bundle adjustment using control lines and tie points, and bundle adjustment using control patches and tie points. The table shows that all used mathematical models resulted in comparable results. In addition, *Model 3* (expanding the error ellipse in the line direction in the object space) and *Model 5* (restricting the weight matrix in the line direction in the object space) produced relatively higher values of root mean square error compared to the other models for lines (*Model 1* to *Model 5*). The reason behind this is that we used different identification codes for the image points along the linear features for each image to compensate for the non-correspondence of line end points in image space, and therefore the images were not tied well. However, the results provided by all used models were still acceptable and comparable.

5. CONCLUSIONS AND RECOMMENDATIONS

This paper presented different approaches for incorporating bot h linear and areal features from LiDAR data in establishing goo d photogrammetric georeferencing. The performance of the pro posed approaches was evaluated using simulated datasets. Exper iments were conducted to simulate the case of both single resect ion and bundle adjustment. The experimental results of both of t he two cases showed that using control linear features and areal features extracted from LiDAR for photogrammetric georeferen

cing led to reliable results. In addition, for bundle adjustment ex periments, expanding the error ellipse and restricting the weight matrix in the object space for linear features using different iden tification codes for the line end points resulted in relatively high er errors in comparison to the other used approaches. However, results were still acceptable.

Future research will focus on the automation of the extraction of linear and areal features from photogrammetric and LiDAR data as well as establishing the correspondence between conjugate primitives. In addition, we will apply the proposed methodologies on line cameras. Moreover, we will study the possibility of using the proposed approaches for both LiDAR and camera calibration. Furthermore, we will utilize the EOP extracted from the proposed approaches to generate true orthophotos. Finally, we will investigate the development of new visualization tools for an easier portrayal of the registration outcomes such as draping orthophotos on LiDAR data to provide 3D textured models.

ACKNOWLEDGEMENTS

REFERENCES

Baltsavias, E. (1999). A Comparison Between Photogrammetry and Laser Scanning, *ISPRS Journal of Photogrammetry & Rem ote Sensing*, 54(1):83–94.

Chen, L., Teo, T., Shao, Y., Lai, Y., and Rau, J. (2004). Fusion of LIDAR data and optical imagery for building modeling, *Intern ational Archives of Photogrammetry and Remote Sensing*, 35(B 4):732-737.

Cramer, M., Stallmann, D., and Haala, N. (2000). Direct geo-referencing using GPS/Inertial exterior orientations for photogra mmetric applications, *International Archives of Photogrammetr y and Remote Sensing*, 33(B3):198-205.

Fraser, C., and Hanley, H. (2003). Bias compensation in Rationa l Functions for IKONOS Satellite Imagery, *Photogrammetric E ngineering & Remote Sensing,* 69(1): pp. 53-57.

Habib, A., and M. Morgan (2003). Linear features in photogram metry, Invited Paper, *Geodetic Science Bulletin*, 9 (1): 3.

Habib, A., Morgan, M., and Lee, Y. (2002). Bundle adjustment with self-calibration using straight lines, *Photogrammetric Record*, 17(10 0): 635-650.

Habib, A., Morgan, M., Kim, E., and Cheng, R. (2004). Linear Features in Photogrammetric Activities, *ISPRS Congress, Istanb ul, Turkey*, 2004, PS ICWG II/IV: Automated Geo-Spatial Data Production and Updating, pp.610.

Habib, A., Bang, K., Aldelgawy, M., and Shin, S. (2007). Integr ation of Photogrammetric and LiDAR Data in a Multi-primitive Triangulation Procedure, *Proceedings of the ASPRS 2 007*, Tampa, Florida.

Kim C., Habib A., and Mrstik P. (2007). New Approach for Plan ar Patch Segmentation using Airborne Laser Data. *Proceedings of the ASPRS 2007*, Tampa, Florida.